

# Ultrafast vibrational dynamics by time-delayed nondegenerate optical four-wave mixing in condensed matter

M. Aihara

*Department of Physics, Yamaguchi University, Yamaguchi 753, Japan*

M. Hama\*

*Department of Applied Physics, Faculty of Engineering, Osaka City University, Sumiyoshi-ku, Osaka 558, Japan*

(Received 13 February 1995; revised manuscript received 17 April 1995)

Ultrafast dynamical phenomena in an electronic system coupled to the atomic vibrational degrees of freedom of a condensed matter environment are shown to be revealed in time-delayed nondegenerate optical four-wave mixing (OFWM) experiments. We perform a numerical multiple integration and obtain both the time-dependent and time-integrated signal intensity as a function of the time interval  $\tau_s$  between the two excitation light pulses. In contrast to the Markovian relaxation case where the vibrational degrees of freedom simply play the role of a thermal reservoir, our analysis, which takes into consideration the nonequilibrium dynamics of the vibrational system, shows that the time-dependent signal intensity is asymmetric with respect to the positive and negative off-resonance frequency  $\Omega_2$  of the second excitation pulse, even when the first excitation pulse is on resonance. It is also found that the time-integrated intensity measured as a function of  $\tau_s$ , shows a delayed peak which becomes more pronounced as  $\Omega_2$  is decreased. These phenomena are manifestations of the nonequilibrium atomic vibrations generated by the optical excitation and the electron-vibration interaction. It is emphasized that time-delayed nondegenerate OFWM is the most direct and efficient tool for investigating ultrafast dynamics of optically generated nonequilibrium states.

## I. INTRODUCTION

Transient optical four-wave mixing (OFWM) experiments, such as the photon echo<sup>1</sup> and the spatial parametric effects,<sup>2</sup> enable us to investigate ultrafast relaxation dynamics in various kinds of condensed materials.<sup>3-10</sup> Phase relaxation (dephasing) is one of the most important processes which provides us with information on the interaction between the relevant electronic systems and vibrational degrees of freedom (thermal reservoir) of condensed phases. It is well understood that the dephasing phenomenon arises from the random motion of the thermal reservoir, which rapidly modulates the electronic transition frequency and therefore causes degradation of the phase coherence of the quantum superposition between the electronic ground and excited states. For materials in which the interaction between the relevant system and the thermal reservoir is strong, the dephasing time  $T_2$  becomes short. When we consider extremely fast relaxation processes in the femtosecond time regime, we should pay special attention to the fact that phase relaxation can no longer be properly described by  $T_2$ . That is, non-Markovian effects due to thermal reservoir memory play an essential role in transient nonlinear optical phenomena. This was analyzed in Ref. 3.

For an ultrashort time regime comparable to the correlation time  $\tau_c$  of the thermal motion of the reservoir, the effect due to the reservoir cannot simply be regarded as a random frequency modulation, and the dynamical (not stochastic) motion of the reservoir is reflected in transient

nonlinear optical effects such as the photon echo, the spatial parametric effect, pump-probe spectroscopy, and so on. This statement is quite general and is not restricted to a localized-electron phonon system. It is applicable to various kinds of materials, such as inorganic and organic semiconductors, the large molecules embedded in liquid solvents or glasses, disordered systems, and so on. Non-Markovian relaxation manifests itself not merely in the nonexponential decay of the signal intensity, but also in the oscillatory dephasing which directly reflects the dynamics of the reservoir motion.<sup>3</sup> It should be noted that this oscillatory dephasing cannot simply be interpreted as quantum beats. This is because the dephasing and the oscillation are caused by the same degrees of freedom of the reservoir, so that the phenomenon should be interpreted as the non-Markovian effect from the unified viewpoint. When we consider the non-Markovian effect associated with the *nonlinear* optical process, we should note that it is not possible to represent the relaxation behavior by invoking either a distribution of  $T_2$ 's or by a time- or energy-dependent  $T_2$ . This is because one must take into account the correlation between different time intervals, which are separated by the radiation-matter interaction vertices (see Figs. 2 and 3). When the system-reservoir interaction is very strong, this correlation effect gives rise to photon-echo-like phenomena.<sup>11</sup>

Although the first non-Markovian theory of transient OFWM allowed for a pulse of arbitrary shape and duration, the calculation for a localized-electron phonon system was confined to the limiting situation in which the

excitation pulse was short (white spectrum).<sup>3</sup>

In the present paper, we extend this analysis to the more general case in which time-delayed *nondegenerate* OFWM is generated by excitation pulses of arbitrary pulse duration. In condensed matter where extremely fast relaxation occurs, the absorption spectrum is often significantly broadened because of the strong system-reservoir interaction. Therefore, the dependence of the transient OFWM response on the optical excitation frequency provides us with direct and detailed information on the dynamical behavior of optically excited condensed matter. In what follows we analyze the OFWM process taking into account both the excitation time resolution as well as its spectral composition.

## II. SHORT-PULSE LIMIT (REVIEW)

Before going into a detailed analysis, let us briefly review the major results of the earlier non-Markovian theory of transient OFWM.<sup>3</sup> Let us consider transient four-wave mixing caused by a sequence of two laser pulses applied at times 0 and  $\tau_s$  with wave vectors  $\vec{k}_1$  and  $\vec{k}_2$ , respectively. For a sufficiently short excitation pulse the intensity of a response along  $2\vec{k}_2 - \vec{k}_1$  is given, aside from the multiplicative factor, by

$$I^{(3)}(t) = \exp\left[-4S_r(t - \tau_s) - 4_r S(\tau_s) + 2S_r(t)\right], \quad (2.1)$$

where

$$S_r(t) \equiv \text{Re} \int_0^t dt_1 \int_0^{t_1} dt_2 \langle V(t_1) V(t_2) \rangle \quad (2.2)$$

is the real part of the second cumulant. The operator  $V(t)$  in the interaction picture is responsible for the change of the optical transition frequency caused by the system-reservoir interaction, and  $\langle \dots \rangle$  denotes the quantum statistical average. In deriving Eq. (2.1), the higher cumulants are neglected; the validity of this approximation will be discussed later. Formula (2.1) generally describes the exponential dephasing, the oscillatory dephasing, and the photon-echo behavior in the unified manner as is briefly remarked below (see Fig. 1 and Ref. 3). This expression was re-derived by stochastic theory in Ref. 12.

Let us first consider the conventional Markovian case where simple exponential dephasing occurs. The time dependence of  $V(t)$ , which is caused by the reservoir with many degrees of freedom, is usually very rapid and random. If the correlation function  $\langle V(t_1) V(t_2) \rangle$  decays much faster than the observation time  $t$ , the double integral in Eq. (2.2) becomes approximately linear in  $t$ , and we obtain  $S_r(t) \approx t/T_2$  with the dephasing time  $T_2 \equiv (\langle V^2 \rangle \tau_c)^{-1}$ , where  $\tau_c$ , the so-called correlation time, is the measure of the decay of the correlation function. Substituting the above equation in Eq. (2.1), we find the well-known result

$$I^{(3)}(t) \approx e^{-(2/T_2)t}. \quad (2.3)$$

We should here remark that the dephasing time  $T_2$  properly describes the phase relaxation phenomena only when

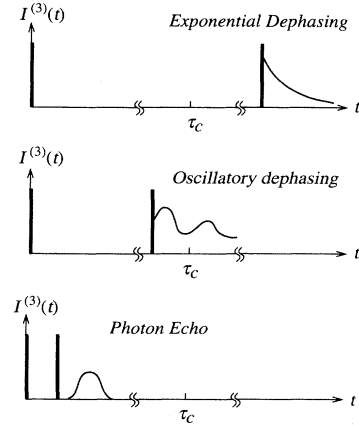


FIG. 1. Qualitative sketch of the transient optical four-wave mixing response in three typical time regions, which are expressed by Eq. (2.1) in the unified manner.

$\tau_c$  is essentially zero. In other words, the dephasing shows exponential temporal decay only on a time scale much longer than  $\tau_c$ .

The formula expressed by Eq. (2.1) describes the general transient four-wave mixing process in condensed matter where  $\tau_c$  can no longer be regarded as being sufficiently short. If the interaction strength between the relevant system and the reservoir is increased, the dephasing becomes fast, and therefore the observation time scale becomes short. If the time scale is comparable with  $\tau_c$ , the frequency modulation by the reservoir can no longer be regarded as a fully random process. The dephasing therefore becomes nonexponential, reflecting the memory effect of the reservoir. It should be stressed that when we consider the ultrafast dephasing phenomena in the femtosecond time scale, this non-Markovian effect should be always taken into consideration, and the dephasing time  $T_2$  becomes meaningless. In such non-Markovian dephasing phenomena, we should also consider the fact that the reservoir system cannot literally be regarded as a thermal bath which always stays in thermal equilibrium; that is, the reservoir is also excited to nonequilibrium states by the coupling with the relevant system under the optical excitation. This effect cannot be analyzed by stochastic theory in which the frequency modulation is merely treated as a stationary random process which is independent of the motion of the relevant system. A typical phenomenon due to the nonequilibrium motion of reservoir is the oscillatory dephasing in a localized-electron phonon system.<sup>3</sup> The phonon system in this case contributes not only to the phase degradation of the relevant electronic system, but also to its dynamic level shift due to the nonequilibrium lattice motion.

Next let us consider the case where the system-reservoir interaction is extremely strong, and therefore the decay of induced polarization is much faster than  $\tau_c$ . In this case, the motion of the reservoir is so slow compared to the decay of induced polarization that the time dependence of modulation of optical transition frequency can be neglected. In this extremely short time scale,

$\langle V(t_1)V(t_2) \rangle$  is approximated to  $\langle V^2 \rangle$ , and so  $S_r(t)$  defined by Eq. (2.2) approximately becomes quadratic in  $t$  as  $S_r(t) \approx \frac{1}{2} \langle V^2 \rangle t^2$ . Substituting this into Eq. (2.1), we find

$$I^{(3)}(t) \approx \exp \left[ -\frac{1}{4} \langle V^2 \rangle (t - 2t_s)^2 \right]. \quad (2.4)$$

The above expression indicates that the photon echo is formed at time  $2\tau_s$ , which was predicted in Ref. 11, and was re-examined by a stochastic model in Refs. 12, 13. Expression (2.4) implies that the very strongly interacting systems is similar to the inhomogeneously broadened systems with the static distribution of transition frequency. For example, in strongly coupled localized-electron phonon systems such as  $F$  centers in alkali halides, the assembly of the vertical Frank-Condon transitions in the configuration coordinate space plays the role of an inhomogenous spectral distribution. The result given by Eq. (2.4) is quite general, and this kind of photon-echo phenomena is expected to be observed in various materials with strong interaction, even when the conventional inhomogenous broadening due to spatial crystalline field inhomogeneity is absent.

### III. ANALYSIS AND RESULTS

Let us consider a two-level quantum system composed of ground and excited states  $|g\rangle$  and  $|e\rangle$ , which interacts with a thermal reservoir composed of many degrees of freedom. Here, it should be noted that the term "thermal reservoir" is used in the wide sense where the finiteness of correlation time (i.e., the memory effect) and the reaction from the relevant two-level system are included. The Hamiltonian of this system is given by

$$H_0 = |g\rangle H_g \langle g| + |e\rangle H_e \langle e| \quad (3.1)$$

$$= H_g + |e\rangle (\varepsilon + V) \langle e|. \quad (3.2)$$

Here, it is assumed that the two levels are well separated so that the direct transition between the two states due to the interaction with the reservoir is neglected. In the above equation,  $H_g$  and  $H_e$  are not the energy eigenvalues of the two-level system, but the operators which include dynamical variables of the reservoir. In Eq. (3.2),  $\varepsilon$  and  $V$  are defined by

$$\varepsilon \equiv \langle (H_e - H_g) \rangle, \quad (3.3)$$

$$V \equiv H_e - H_g - \varepsilon. \quad (3.4)$$

Here and henceforth,

$$\langle \dots \rangle \equiv \text{Tr}_{(r)} (\dots \rho_{eq}) \quad (3.5)$$

denotes the quantum statistical average over the reservoir states in thermal equilibrium, where

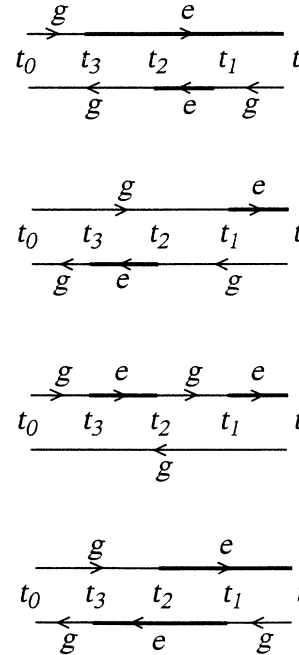


FIG. 2. Diagrams for the third-order nonlinear optical processes which contribute to  $\langle e | \rho^{(3)}(t) | g \rangle$ . The thin and thick lines are associated with the excited and ground tates of the relevant system, respectively.

$$\rho_{eq} \equiv \left( \text{Tr}_{(r)} (e^{-\beta H_g}) \right)^{-1} e^{-\beta H_g} \quad (3.6)$$

is the equilibrium statistical operator for the reservoir in the ground-state manifold, and the thermal population in the upper level  $|e\rangle$  is assumed to be negligibly small. The operator  $V$  defined by Eq. (3.4) describes the change of the energy separation between  $|g\rangle$  and  $|e\rangle$  which is caused by the interaction with the reservoir. The Hamiltonian of this matter system interacting with the coherent radiation is given by

$$\tilde{H}(t) = H_0 + H_1(t), \quad (3.7)$$

$$H_1(t) = -|g\rangle \mu \langle e| E^*(\vec{r}, t) - |e\rangle \mu^* \langle g| E(\vec{r}, t), \quad (3.8)$$

where  $E(\vec{r}, t)$  is the complex amplitude of the radiation field, and  $\mu$  is the transition moment which is assumed to be independent of reservoir variables (Condon approximation); their vector notation is omitted for simplicity. In the above expression, the rotating-wave approximation is used.

Expectation values of observables associated with the third-order optical nonlinearity are obtained by the third-order perturbation term for the statistical operator (density operator), which has the form (here and henceforth we set  $\hbar = 1$ )

$$\rho^{(3)}(t) = i \int_{t_0}^t dt_1 \int_{t_0}^{t_1} dt_2 \int_{t_0}^{t_2} dt_3 e^{-iL_0(t-t_1)} L_1(t_1) e^{-iL_0(t_1-t_2)} L_1(t_2) e^{-iL_0(t_2-t_3)} L_1(t_3) \rho(t_0). \quad (3.9)$$

Here, the Liouville operators  $L_0$  and  $L_1(t)$  are defined by  $L_0 \cdots \equiv [H_0, \cdots]$  and  $L_1(t) \cdots \equiv [H_1(t), \cdots]$ , respectively. The above equation implies that matter interacts with radiation 3 times at  $t_1$ ,  $t_2$ , and  $t_3$ .

The nonlinear polarization is given by the off-diagonal element of  $\rho^{(3)}(t)$  as

$$P^{(3)}(t) \equiv \text{Tr} \left[ \left( \mu |g\rangle\langle e| + \mu^* |e\rangle\langle g| \right) \rho^{(3)}(t) \right] \\ = \mu \text{Tr}_{(r)} \left( \langle e | \rho^{(3)}(t) | g \rangle \right) + \text{c.c.} \quad (3.10)$$

Figure 2 shows the schematic representation of  $\langle e | \rho^{(3)}(t) | g \rangle$ . It is assumed that the system starts out at  $t_0$  in the ground state  $|g\rangle$ . The pair of upper and lower lines corresponds to the two states associated with the matrix element of  $\rho(t)$ , respectively. For example, the first diagram in Fig. 2 describes the following third-order nonlinear optical process: The initial element  $\langle g | \rho^{(0)} | g \rangle$  is transferred to  $\langle g | \rho^{(1)} | e \rangle$  at  $t_3$ , it is transferred to  $\langle e | \rho^{(2)} | e \rangle$  at later time  $t_2$ , and finally it is transferred to  $\langle e | \rho^{(3)} | g \rangle$  at time  $t_1$ . The reason for the opposite direc-

tion of the time arrows for upper and lower lines is that the roles of the excitation operator  $S^\dagger \equiv |e\rangle\langle g|$  and the deexcitation operator  $S \equiv |g\rangle\langle e|$  are interchanged when operating on ket and bra spaces; that is, for example, both  $S^\dagger |g\rangle = |e\rangle$  in the ket space and  $\langle g| S = \langle e|$  in the bra space correspond to the excitation process.

The electric field representing two excitation pulses separated by  $\tau_s$  is given by

$$E(\vec{r}, t) = E_1(t) e^{i(\vec{k}_1 \cdot \vec{r} - \Omega_1 t)} + E_2(t - \tau_s) e^{i(\vec{k}_2 \cdot \vec{r} - \Omega_2 t)}. \quad (3.11)$$

Let us focus our attention on the signal emitted along the direction  $2\vec{k}_2 - \vec{k}_1$ , which is represented by the diagrams shown in Fig. 3. When we consider the case for which the two excitation pulses are temporally well separated, i.e., when the overlap between  $E_1(t)$  and  $E_2(t)$  can be neglected, then the contribution of the first and second diagrams can be neglected. Because in many condensed materials the induced polarization decays much faster than the lifetime of the excited state, the third and fourth diagrams can be combined to yield

$$\langle e | \rho^{(3)}(t) | g \rangle = i\mu(\mu^*)^2 \int_{t_0}^t dt_1 \int_{t_0}^t dt_2 \int_{t_0}^{\text{Min}(t_1, t_2)} dt_3 E(\vec{r}, t_1) E(\vec{r}, t_2) E^*(\vec{r}, t_3) \\ \times e^{-iH_e(t-t_1)} e^{-iH_g(t_1-t_3)} \rho_{\text{eq}} e^{iH_e(t_2-t_3)} e^{iH_g(t-t_2)}. \quad (3.12)$$

With the use of the formula for the time-ordered exponential

$$\exp_+ \left[ -i \int_{t_0}^t dt' V(t') \right] = e^{iH_g t} e^{-i(H_g + V)(t-t_0)} e^{-iH_g t_0}, \quad (3.13)$$

with  $V(t) \equiv \exp(iH_g t) V \exp(-iH_g t)$ , the average of the product of the four exponential operators in Eq. (3.12) can be evaluated by the cumulant expansion to yield

$$\ln \left\langle e^{iH_e(t_2-t_3)} e^{iH_g(t-t_2)} e^{-iH_e(t-t_1)} e^{-iH_g(t_1-t_3)} \right\rangle \approx -i\varepsilon(t-t_1-t_2+t_3) + S(t-t_3)^* - S(t_2-t_3)^* \\ - S(t_1-t_3)^* - S(t-t_1) - S(t-t_2)^* + S(t_1-t_2)^*. \quad (3.14)$$

Here

$$S(t) \equiv \int_0^t dt_1 \int_0^{t_1} dt_2 \langle V(t_1) V(t_2) \rangle = \int_{-\infty}^{\infty} \frac{d\omega}{2\pi} \frac{J(\omega)}{\omega^2} (1 - e^{-i\omega t}) \quad (3.15)$$

is the second-cumulant (the higher-order cumulants have been neglected) and  $J(\omega)$  is the power spectrum (the interaction spectral function) defined by

$$J(\omega) = \int_{-\infty}^{\infty} dt e^{i\omega t} \langle V(t) V(0) \rangle. \quad (3.16)$$

The second-cumulant approximation expressed by Eq. (3.15) is generally valid as long as the coupling between the two-level system and the reservoir is sufficiently weak. We should, however, remark that, irrespective of the coupling strength, Eq. (3.14) is exact for a linearly coupled system where  $V$  is a linear function of the vibration amplitudes for reservoir variables, as in the case of a linearly coupled localized-electron phonon system. In many cases the quadratic and higher-order coupling is much weaker than the linear one. It follows that (3.14) may be widely applicable to various kinds of materials.

From Eqs. (3.10)–(3.15), we obtain the expression for the nonlinear polarization generated by the two-pulse excitation:

$$P^{(3)}(t) = i|\mu|^4 e^{-i\varepsilon t} \int_{t_0}^t dt_1 \int_{t_0}^t dt_2 \int_{t_0}^{\text{Min}(t_1, t_2)} dt_3 E_2(t_1) E_2(t_2) E_1(t_3)^* \exp[i(\varepsilon - \Omega_2)(t_1 + t_2) - i(\varepsilon - \Omega_1)t_3] \\ \times \exp[S(t-t_3)^* - S(t_2-t_3)^* - S(t_1-t_3)^*] \exp[-S(t-t_1) - S(t-t_2)^* + S(t_1-t_2)^*] + \text{c.c.}, \quad (3.17)$$

and the time dependence of the signal intensity is given by

$$I^{(3)}(t) = |P^{(3)}(t)|^2. \quad (3.18)$$

For extremely fast phenomena, the observable quantity of interest is the time-integrated signal intensity

$$I_{\text{in}}^{(3)}(\tau_s) = \int_{-\infty}^{\infty} dt I^{(3)}(t), \quad (3.19)$$

which is to be calculated as a function of  $\tau_s$ .

We are now in a position to perform the numerical integration in Eqs. (3.17) and (3.19) for a specific model. In order to confine our attention to the transient OFWM response associated with the extremely fast vibrational relaxation behavior found in condensed matter at low temperatures, we consider a two-level electronic system which is interacting with many vibrational degrees of freedom; a typical example is the localized-electron phonon system. We model the power spectrum (3.16) by

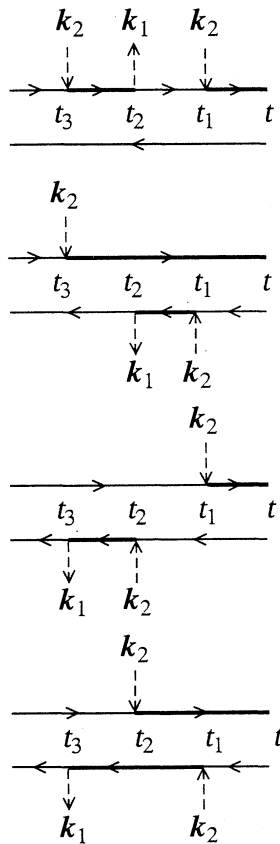


FIG. 3. Diagrams associated with the four-wave mixing signal light with the wave vector  $2\vec{k}_2 - \vec{k}_1$ . A down and up arrows in the diagrams are, respectively, associated with the factor  $\exp(i\vec{k} \cdot \vec{r})$  and  $\exp(-i\vec{k} \cdot \vec{r})$ , which correspond to the photon absorption and emission processes for the upper-side lines (with right arrows); note that the meaning of absorption and emission is interchanged for the lower-side lines (with left arrows).

$$\Omega_1 = 0 \quad \Omega_2 = 0$$

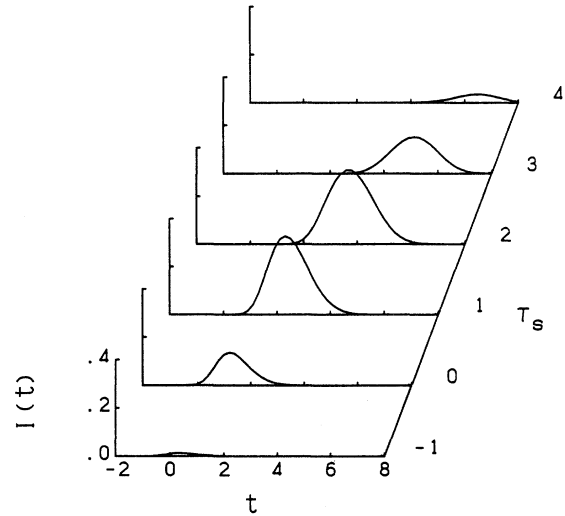


FIG. 4. The time dependence of the signal radiation intensity for several values of the time interval  $\tau_s$  between two excitation optical pulses. The average vibrational frequency  $\omega_r$  and the width  $\gamma_r$  of the vibrational frequency distribution are, respectively, set to 0.1 and 0.01 in units of  $\delta = 1$  [see Eq. (3.21)].

$$J(\omega) = \frac{\sqrt{\pi} S}{\gamma_r} \omega^2 \exp\left(-\frac{(\omega - \omega_r)^2}{4\gamma_r^2}\right), \quad (3.20)$$

where  $S$  is the dimensionless coupling constant,  $\omega_r$  is the average vibrational frequency,  $\gamma_r$  is the width of the vibrational frequency distribution, and  $\gamma_r^{-1}$  is the measure of the correlation time  $\tau_c$ . At finite temperatures, the

$$\tau_s = 4 \quad \Omega_1 = 0$$

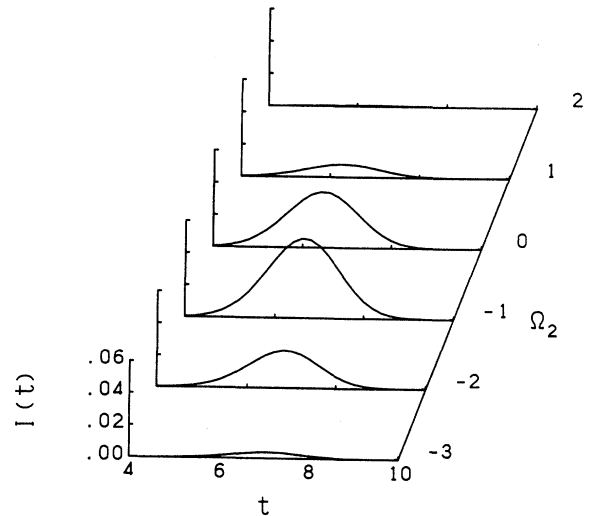


FIG. 5. The time dependence of the signal radiation intensity for several values of frequency  $\Omega_2$  of the second excitation optical pulse. The average vibrational frequency  $\omega_r$  and the width  $\gamma_r$  of the vibrational frequency distribution are, respectively, set to 0.1 and 0.01 in units of  $\delta = 1$  [see Eq. (3.21)].

quadratic electron-vibration interaction produces weak peaks in  $J(\omega)$  around  $2\omega_r$ ,  $0$ , and  $-2\omega_r$  as is shown in Ref. 3. The middle peak near zero frequency is responsible for the long-time exponential tail in the OFWM signal. However, the quadratic electron-vibration interaction has a negligibly small effect in strongly interacting electron-vibration systems where the ultrafast vibrational dynamics predominates the OFWM phenomena. The temporal profile of the excitation pulses is assumed to be Gaussian,

$$E_{1,2}(t) \propto \exp(-\delta^2 t^2). \quad (3.21)$$

In the following numerical examples, we set  $\delta = 1$ . When we calculate the OFWM signal intensity in condensed matter with wide absorption spectra due to a strong system-reservoir interaction, the integrand in Eq. (3.17) is highly oscillatory even in the resonance case. The conventional numerical integration method therefore does not work well. In the present work, we use the special numerical integration method based on the Chebyshev series expansion developed by Hasegawa and Torri.<sup>14</sup>

The time dependence of the signal intensity, Eq. (3.17), for several values of pulse separation is displayed in Fig. 4. The first pulse is applied at time 0, and the second

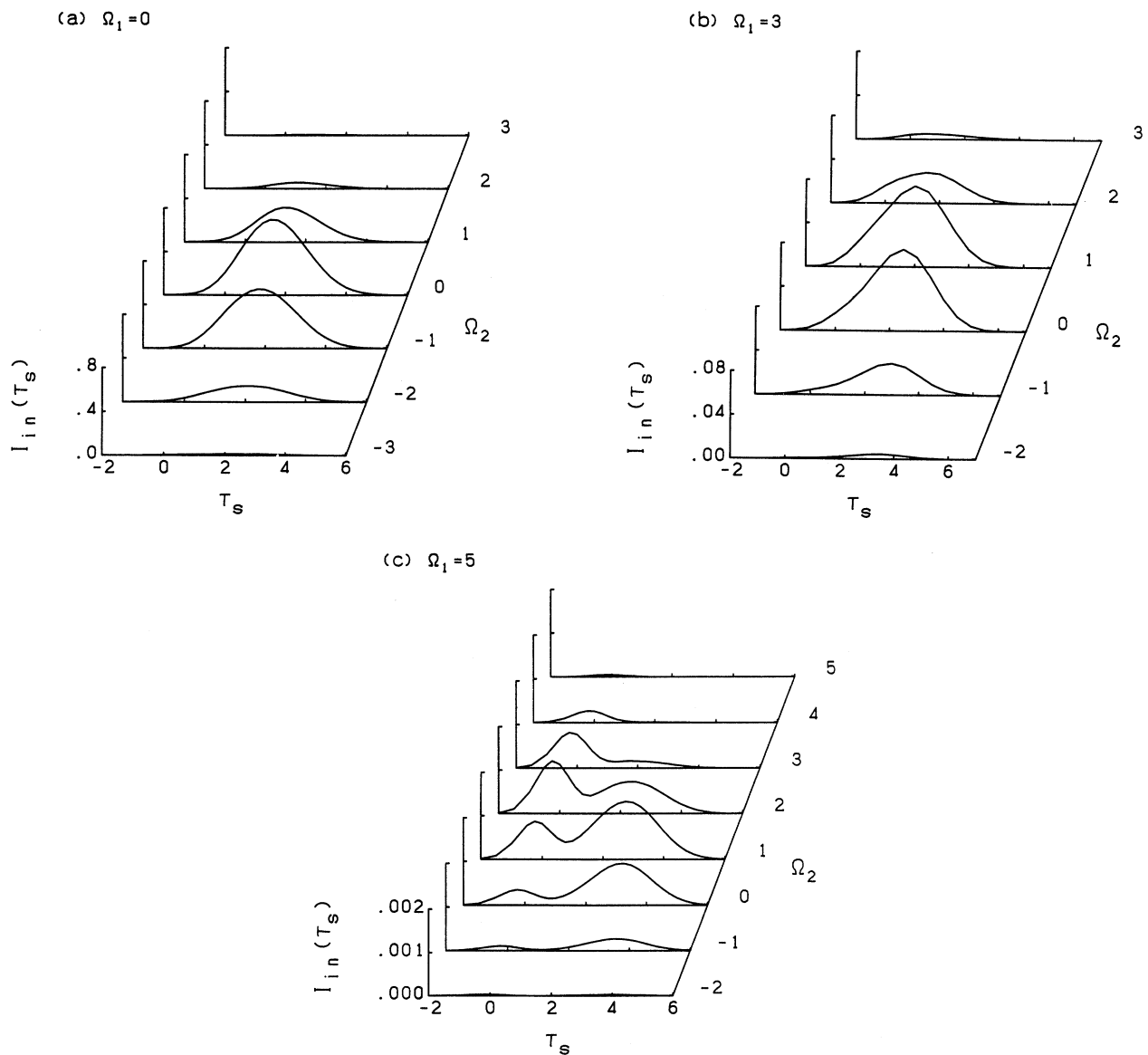
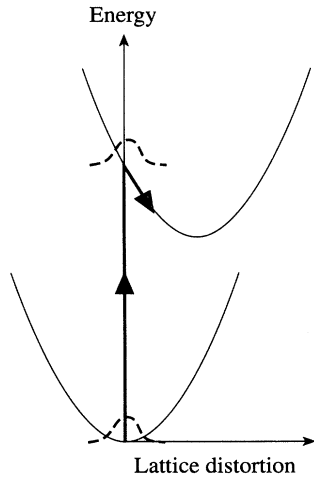


FIG. 6. The dependence of the time-integrated signal radiation intensity on the time interval  $\tau_s$  between two excitation optical pulses for several values of the frequency  $\Omega_2$  of the second excitation optical pulse. The average vibrational frequency  $\omega_r$  and the width  $\gamma_r$  of the vibrational frequency distribution are, respectively, set to 0.1 and 0.01 in units of  $\delta = 1$  [see Eq. (3.21)].

pulse is applied at  $\tau_s$ . In order to investigate the strong coupling case, the dimensionless coupling constant  $S$  in Eq. (3.20) is set at 100, a typical value for  $F$  centers in alkali halides. The incident photon energies  $\Omega_1$  and  $\Omega_2$  for the first and second excitation pulses are measured from the electronic excitation energy  $\varepsilon$ , and so zero energy corresponds to exact resonance. From this figure, we find that in a strongly coupled system the photon-

(a) Resonant excitation



(b) Off-resonant excitation

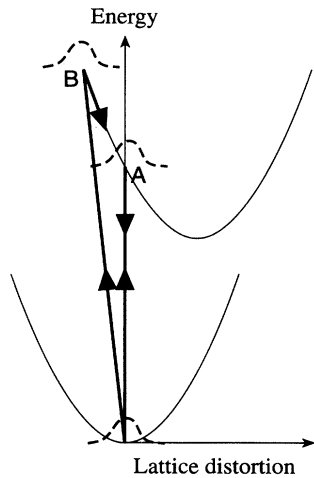


FIG. 7. Schematic representation of the optical excitation process in the configuration coordinate space in the resonance and off-resonance cases. Two parabolic lines represent the adiabatic potential curves associated with two levels  $|g\rangle$  and  $|e\rangle$ . The bell-shaped dashed curves represent the vibrational wave function. The vertical lines with an arrow indicate the optical transition by the first excitation pulse, and the arrow along the potential curve implies the movement of the wave function after the excitation.

echo-like phenomenon arises without the requirement for “inhomogeneous” broadening in the conventional sense as was mentioned in the previous section.<sup>11</sup> For the present model expressed by Eq. (3.20), the shortest time scale for reservoir motion is  $\omega_r^{-1}$ , and the echo phenomenon disappears in the time region longer than  $\omega_r^{-1}$ . The echo decay and the deviation of the echo peak from  $t = 2\tau_s$  provide us with direct information about the nonequilibrium reservoir dynamics. The time dependence of the signal intensity for  $\tau_s = 4$  and for several values of the mean frequency  $\Omega_2$  is shown in Fig. 5. We should note that the profile is highly asymmetric with respect to the positive and negative  $\Omega_2$ , even though the first excitation pulse is exactly resonant ( $\Omega_1 = 0$ ). Because the transient four-wave mixing signal in the direction of  $2\vec{k}_2 - \vec{k}_1$  directly traces the coherence of the system, the above fact implies that the initial coherent polarization associated with the Franck-Condon state with energy  $\varepsilon$  is transferred to lower electron-vibration (vibronic) states in configuration coordinate space, as schematically shown by the downward arrow in Fig. 7(a). This should be contrasted to the so-called spectral diffusion (cross relaxation) which is simply described by the incoherent rate equations for the occupation probabilities (populations).

Nonequilibrium reservoir dynamics in condensed phases, such as the lattice relaxation in a localized-electron phonon system, usually arises in the femtosecond time scale, so that it may be difficult to directly observe it by tracing the time dependence of the signal intensity. It should be emphasized that time-delayed *nondegenerate* OFWM enables us to obtain information on ultrafast vibrational relaxation by looking at the time-integrated intensity  $I_{in}(\tau_s)$  as a function of the pulse separation  $\tau_s$ , for several values of the frequency  $\Omega_2$  of the second excitation pulse, as is shown in Figs. 6. Figure 6(a) shows the case for which the first pulse is on resonance ( $\Omega_1 = 0$ ). We then find that  $I_{in}(\tau_s)$  is larger on the negative side of  $\Omega_2$ . We also find that with decreasing  $\Omega_2$  the peak of  $I_{in}(\tau_s)$  shifts to larger  $\tau_s$ . These results are similar to those in Fig. 5 if we replace the real time  $t$  with the time interval  $\tau_s$ , and they reflect the dynamical motion of the reservoir which results in the coherence transfer of the optically induced polarization to the lower vibronic states in the excited-state manifold associated with  $|e\rangle$ . It should be noted that optically generated coherence of matter is partially preserved during the vibrational relaxation as mentioned before. The above-mentioned peak shift of  $I_{in}(\tau_s)$  with decreasing  $\Omega_2$  can be more clearly observed in the case where the first excitation pulse excites upper vibronic states ( $\Omega_1 > 0$ ), as shown in Fig. 6(b). This delayed generation of coherent polarization should be contrasted with conventional OFWM where the integrated intensity  $I_{in}(\tau_s)$  is a monotonically decreasing function of  $\tau_s$ . It should be emphasized again that this frequency dependence is the distinctive advantage of the nondegenerate transient four-wave mixing over that for the short-pulse limit in which the excitation light frequency is uncertain.

When  $\Omega_1$  is further increased, a double-peak transient response appears, as shown in Fig. 6(c). This interesting transient phenomenon can be explained as follows. In

the case of off-resonance excitation, the following two optical transitions are predominantly induced by the first excitation pulse [see Fig. 7(b)]. The first predominant transition is to the Franck-Condon state *A* with the excitation energy  $\varepsilon$  which has the largest transition dipole moment (i.e., the maximum wave-function overlap with the ground state). Because this transition is significantly off resonant, the excited state promptly (i.e., within the very short time  $(30\omega_r)^{-1}$ ) returns to the ground state to satisfy energy conservation, as indicated by the downward arrow from *A*. This is called the *virtual* transition. As a result, the excited state can be occupied only during the optical excitation, and therefore the polarization of the system temporally follows the excitation pulse profile. The first peak in Fig. 6(c) arises from this *virtual* excitation to the Franck-Condon state. In contrast to this, the second predominant transition is to

the resonantly excited state *B* with the excitation energy  $\varepsilon + 30\omega_r$ . The second peak in Fig. 6(c) is caused by this *real* transition which is followed by the dynamical motion of reservoir variables mentioned in previous figures. With increasing the off-resonance frequency, the ratio of the first prompt component to the second one increases. The above-mentioned intriguing phenomenon associated with the virtual and real transitions is closely related to the competition between scattering and luminescence in transient resonant light scattering.<sup>15</sup>

#### ACKNOWLEDGMENT

The author is sincerely grateful to S. R. Hartmann for a critical reading of the manuscript.

\* Present address: Hannan University, Matsubara, Osaka 580, Japan.

<sup>1</sup> I. D. Abella, N. A. Kurnit, and S. R. Hartmann, *Phys. Rev.* **141**, 391 (1966).

<sup>2</sup> T. Yajima and Y. Taira, *J. Phys. Soc. Jpn.* **47**, 1620 (1979).

<sup>3</sup> M. Aihara, *Phys. Rev. B* **25**, 53 (1982).

<sup>4</sup> J.-Y. Bigot, M. T. Portella, R. W. Schoenlein, C. J. Bardeen, A. Migus, and C. V. Shank, *Phys. Rev. Lett.* **66**, 1138 (1991); R. W. Schoenlein, D. M. Mittleman, J. J. Shiang, A. P. Alivisatos, and C. V. Shank, *ibid.* **70**, 1014 (1993); J.-Y. Bigot, A. Daunois, J. Oberlé, and J.-C. Merle, *ibid.* **71**, 1820 (1993); D. M. Mittleman, R. W. Schoenlein, J. J. Shiang, V. L. Colvin, A. P. Alivisatos, and C. V. Shank, *Phys. Rev. B* **49**, 14435 (1994).

<sup>5</sup> Erik T. J. Nibbering, Douwe A. Wiersma, and Koos Duppen, *Phys. Rev. Lett.* **66**, 2464 (1991).

<sup>6</sup> S. Saikan, T. Nakabayashi, Y. Kanematsu, and A. Imaoka, *J. Chem. Phys.* **89**, 4609 (1988); S. Saikan, T. Nakabayashi, Y. Kanematsu, and N. Tato, *Phys. Rev. B* **38**, 7777 (1988); S. Saikan, A. Imaoka, Y. Kanematsu, K. Sakoda, K. Kominami, and M. Iwamoto, *ibid.* **41**, 3185 (1992); S. Saikan, J. W.-I. Lin, and H. Nemoto, *ibid.* **46**, 11125 (1992); S.

Saikan, *J. Lumin.* **53**, 147 (1992).

<sup>7</sup> F. Minami, A. Hasegawa, S. Asaka, and K. Inoue, *J. Lumin.* **45**, 409 (1990); A. Hasegawa, F. Minami, S. Asaka, and K. Inoue, *ibid.* **45**, 192 (1990); F. Minami, A. Hasegawa, T. Kuroda, and K. Inoue, *ibid.* **53**, 371 (1992).

<sup>8</sup> A. Lohner, K. Rick, P. Leisching, A. Leitenstorfer, and T. Elsaesser, *Phys. Rev. Lett.* **71**, 77 (1993); A. Leitenstorfer, A. Lohner, K. Rick, P. Leisching, T. Elsaesser, T. Kuhn, F. Rossi, W. Stolz, and K. Ploog, *Phys. Rev. B* **49**, 16372 (1994).

<sup>9</sup> Tzzy-Schiuan Yang, R. Zhang, and A. B. Myers, *J. Chem. Phys.* **100**, 8573 (1994).

<sup>10</sup> M. D. Webb, S. T. Cundiff, and D. G. Steel, *Phys. Rev. Lett.* **66**, 934 (1991).

<sup>11</sup> M. Aihara, *Phys. Rev. B* **21**, 2051 (1980).

<sup>12</sup> Shaul Mukamel, *Chem. Phys. Lett.* **114**, 426 (1984).

<sup>13</sup> W. B. Bosma, Y. J. Yan, and Shaul Mukamel, *Phys. Rev. A* **42**, 6920 (1990).

<sup>14</sup> T. Hasegawa and T. Torii, *J. Comput. Appl. Math.* **17**, 21 (1987).

<sup>15</sup> M. Aihara and A. Kotani, *Solid State Commun.* **46**, 751 (1983); M. Aihara, *Phys. Rev. Lett.* **57**, 463 (1986).